Supporting information

Construction and optimization of multi-interfaces nanotube structured phosphorus-doped bimetallic oxides arrays as efficient electrocatalysts for water splitting

Jie Wang, Peng Chen, Shengnan Ruan, Rongmei Liu and Fengcui Shen*

School of Chemical and Environmental Engineering, Anhui Polytechnic University, Wuhu, 241000, P. R. China.

**To whom all correspondence should be addressed*
E-mail: fcshen@ahpu.edu.cn

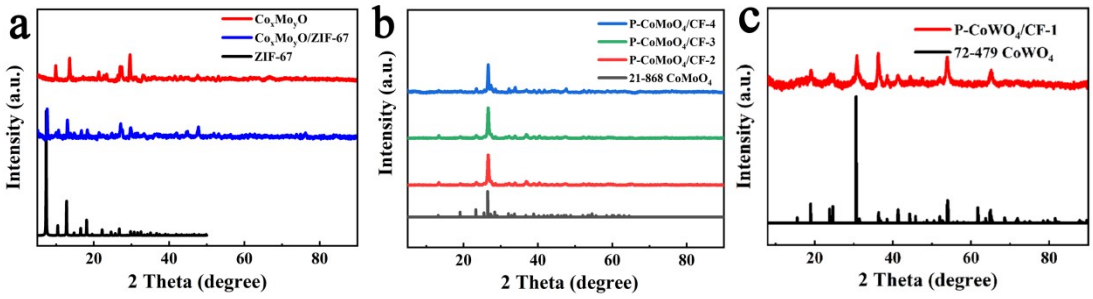

Fig. S1. XRD patterns of (a) CoMo oxide precursors Co_xMo_yO and soaked 2-methylimidazole Co_xMo_yO/ZIF-67, (b) P-$CoMoO_4$/CF-2, 3, 4 and (c) P-$CoWO_4$/CF-1 arrays.

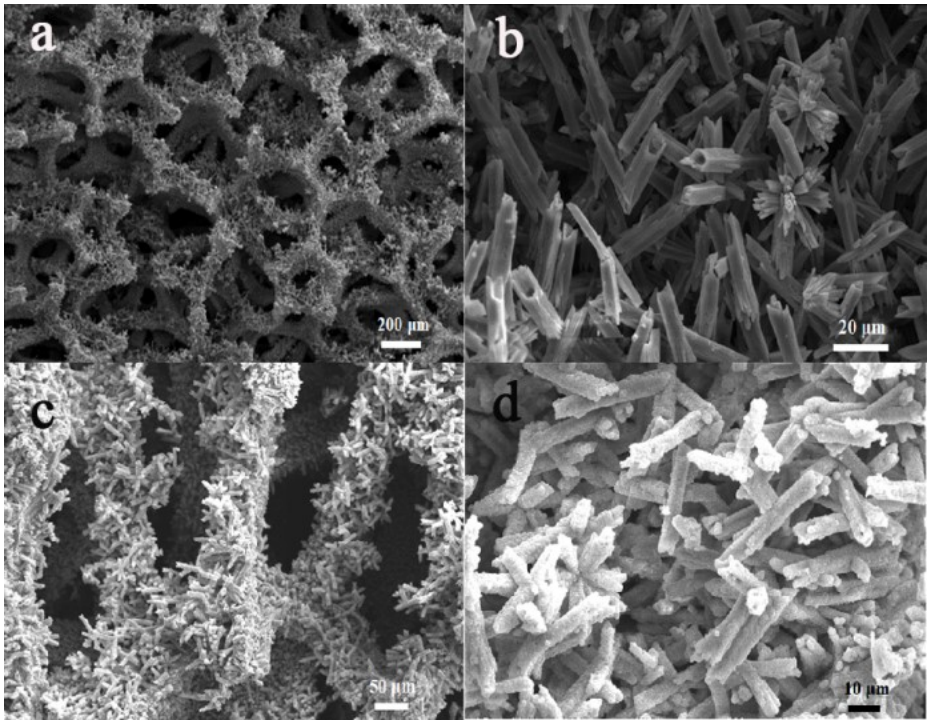

Fig. S2. SEM images of P-$CoMoO_4$/CF-1 (a, b) precursors at different magnifications, (c, d) precursors after immersion in 2-methylimidazole at different magnifications.

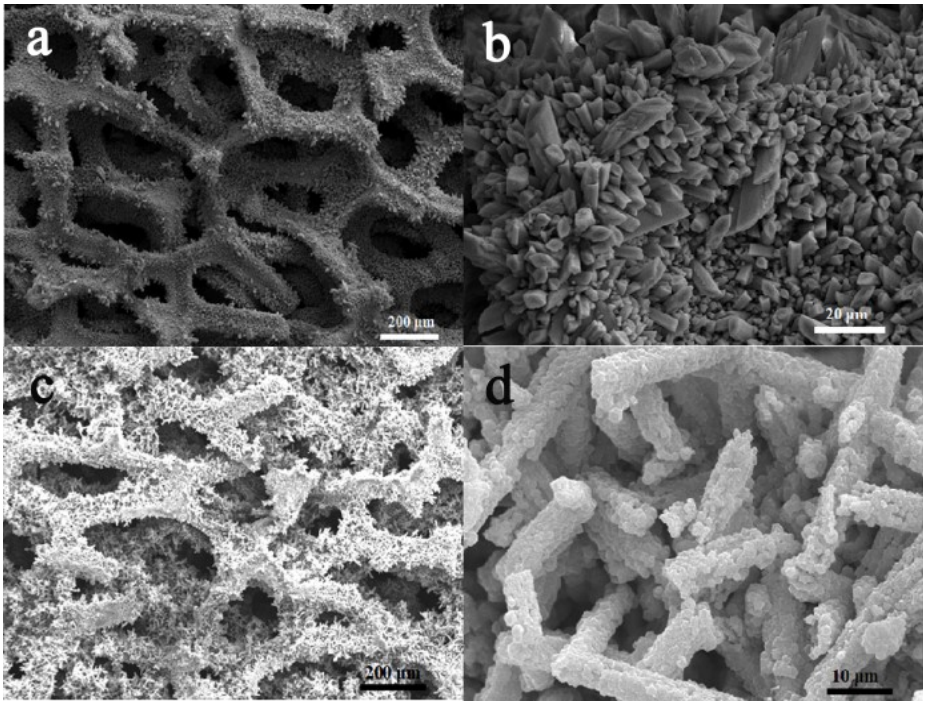

Fig. S3. SEM images of P-$CoMoO_4$/CF-2 (a, b) precursors at different magnifications, (c, d) precursors after immersion in 2-methylimidazole at different magnifications.

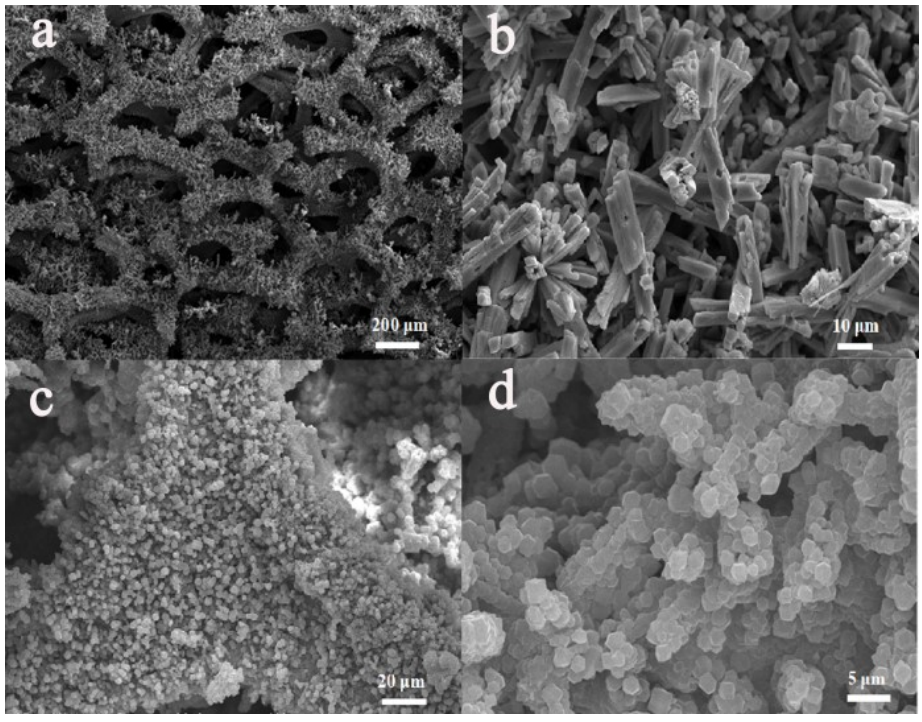

Fig. S4. SEM images of P-$CoMoO_4$/CF-3 (a, b) precursors at different magnifications, (c, d) precursors after immersion in 2-methylimidazole at different magnifications.

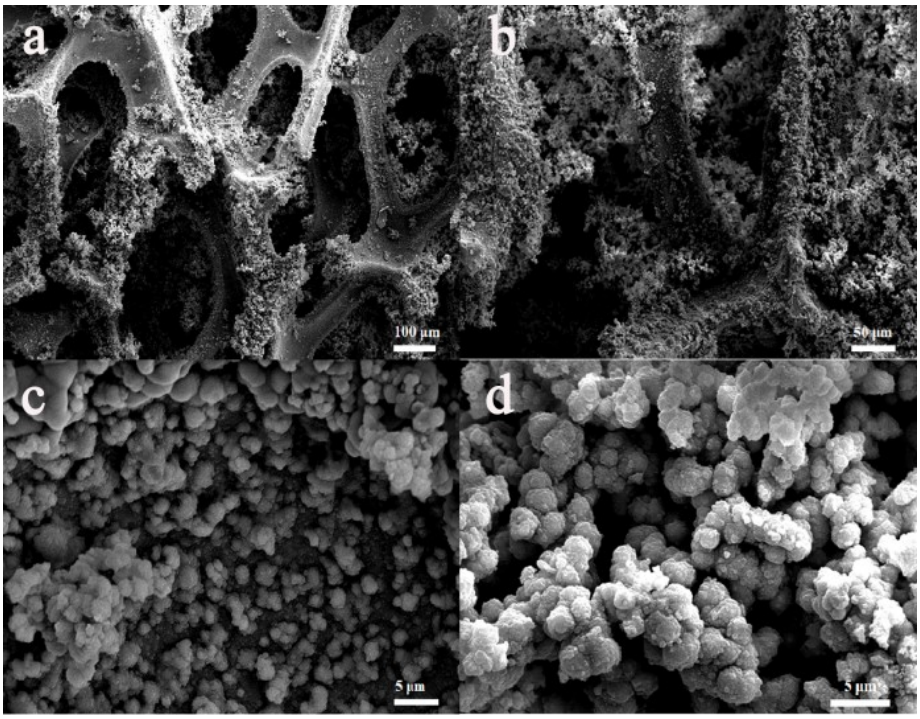

Fig. S5. SEM images of P-$CoMoO_4$/CF-4 (a, b) precursors at different magnifications, (c, d) precursors after immersion in 2-methylimidazole at different magnifications.

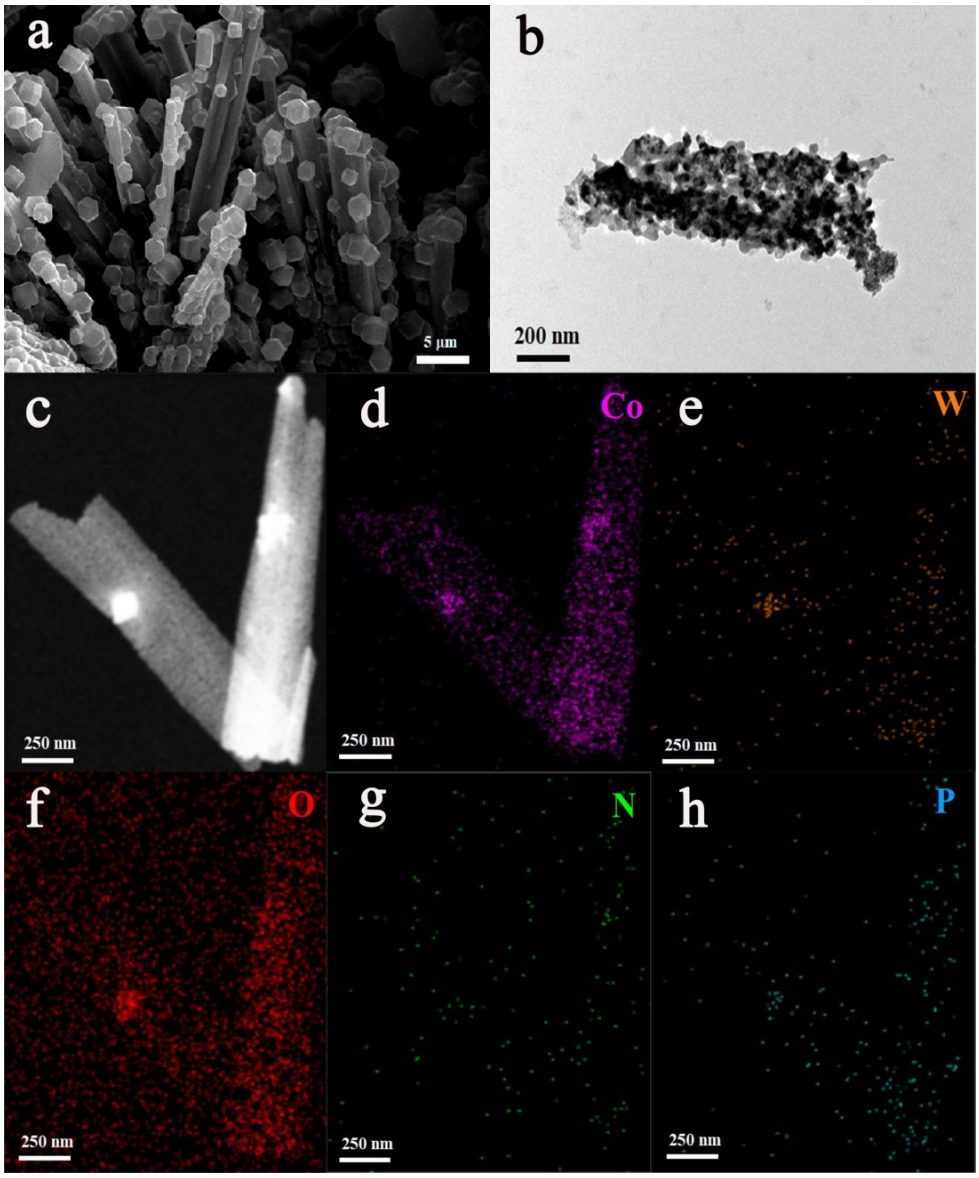

Fig. S6. Characterization of the nanotube array P-$CoWO_4$/CF-1. (a) SEM images of the material, (b) TEM image of P-$CoWO_4$/CF-1, (c-h) elemental mapping (EDX) of P-$CoWO_4$/CF-1.

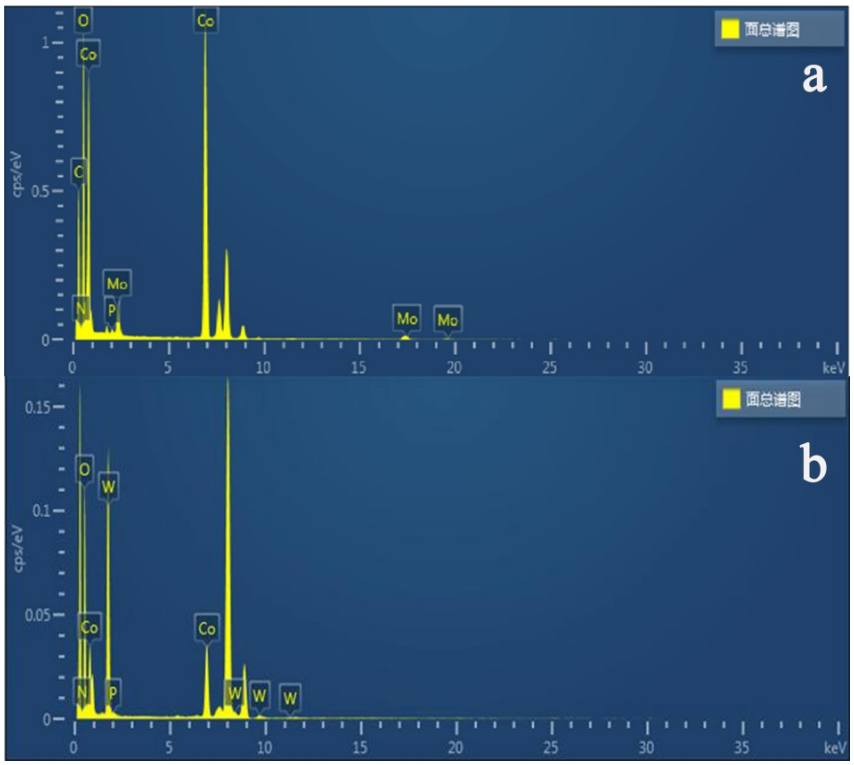

Fig. S7. EDS spectrum of (a) P-$CoMoO_4$/CF-1 arrays and (b) P-$CoWO_4$/CF-1 arrays.

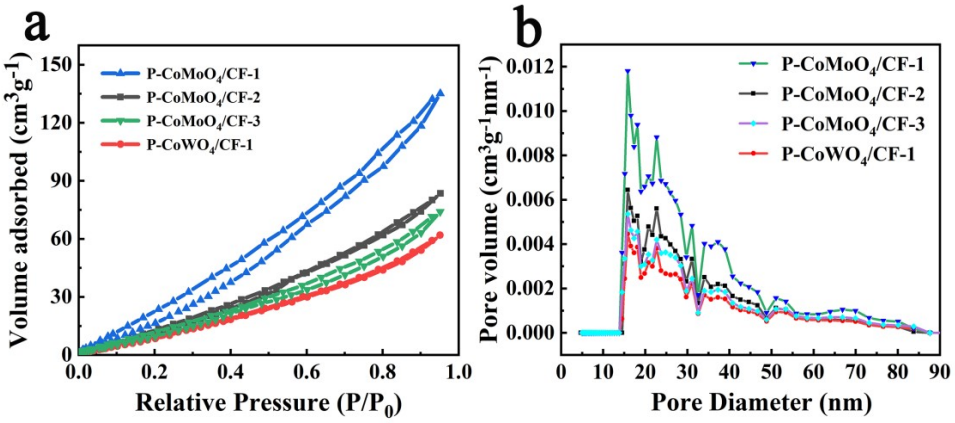

Fig. S8. N_2 adsorption-desorption isotherms and pore size distribution of samples (a) N_2 adsorption desorption isotherms of P-$CoMoO_4$/CF-1, P-$CoMoO_4$/CF-2, P-$CoMoO_4$/CF-3 and P-$CoWO_4$/CF-1, (b) pore size distributions of the synthetic samples.

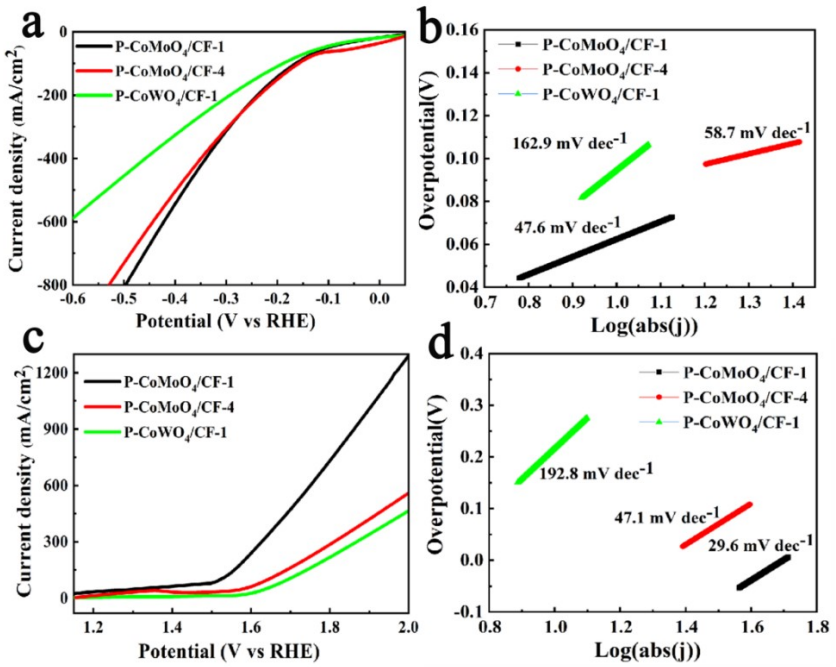

Fig. S9. Electrochemical properties of the electrocatalyst. (a) LSV in HER and (b) polarization curves of Tafel corresponding to catalyst HER, (c) LSV in OER and (d) polarization curves of Tafel corresponding to catalyst OER.

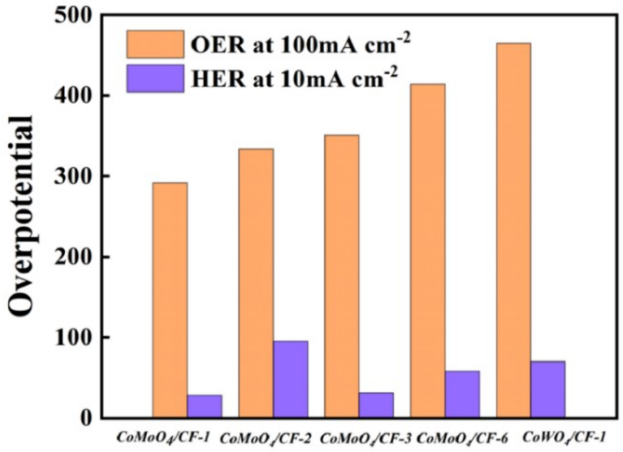

Fig. S10. Comparison of the overpotential of HER at 10mA/cm^2 and OER at 100 mA/cm^2 for the prepared samples.

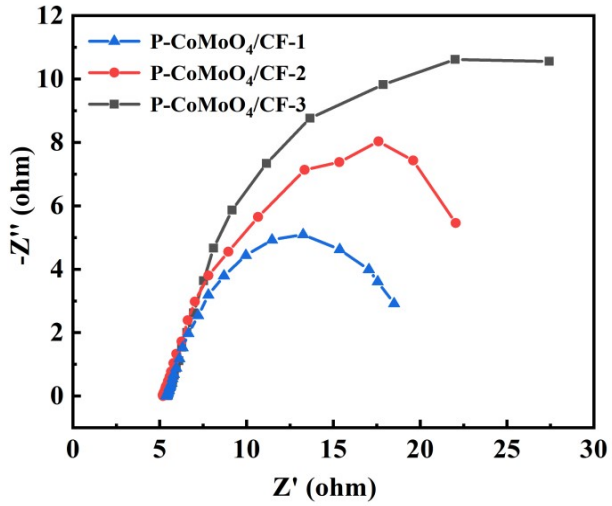

Fig. S11. Electrochemical impedance spectroscopy tests. Nyquist plots of P-$CoMoO_4$/CF-1, P-$CoMoO_4$/CF-2 and P-$CoMoO_4$/CF-3.

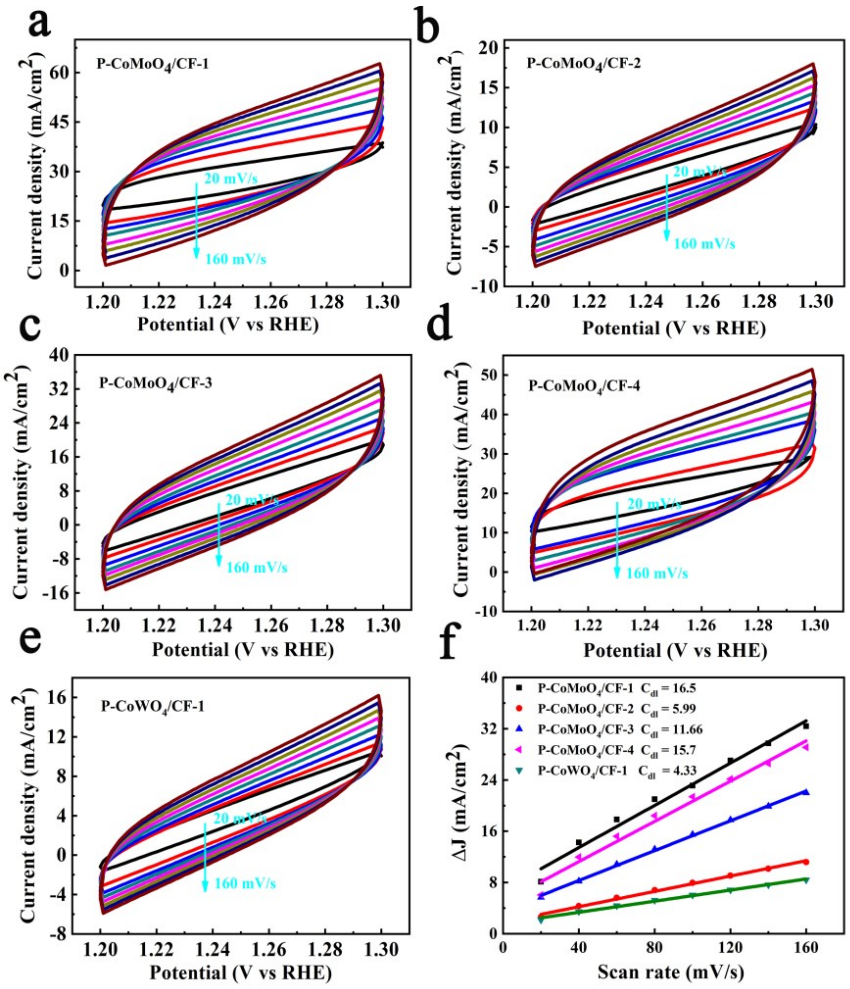

Fig. S12. The electrochemically active specific surface areas of different catalysts. (a), (b), (c) CV of P-$CoMoO_4$/CF-1, P-$CoMoO_4$/CF-2 and P-$CoMoO_4$/CF-3 at different rates from 20 to 160 mV^{-1}, (d), (e) CV of catalysts $CoMoO_4$/CF-4, $CoWO_4$/CF-1 and (f) ΔJ of these catalysts.

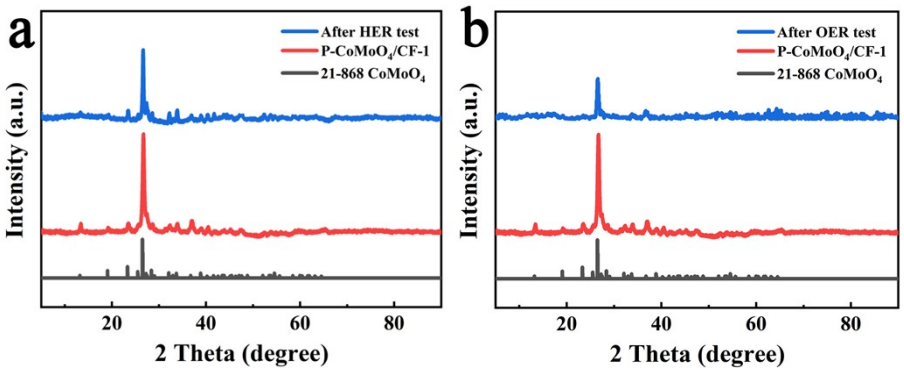

Fig. S13. XRD of the P-$CoMoO_4$/CF-1 samples (a) after HER test, (b) after OER test